**Supporting Information**

# Nanoscale Mechanism of Molecular Transport through the Nuclear Pore Complex as Studied by Scanning Electrochemical Microscopy

Jiyeon Kim, Anahita Izadyar,† Nikoloz Nioradze, and Shigeru Amemiya*

*Department of Chemistry, University of Pittsburgh, Pittsburgh, PA 15260, USA*

* To whom correspondence should be addressed. E-mail: amemiya@pitt.edu.

† Present address: Department of Chemistry and Physics, Arkansas State University, State University, Arkansas, 72467

**Microscopic Characterization of the Isolated Nucleus.** The nucleus was isolated from a *Xenopus laevis* oocyte and characterized microscopically. The large nucleus (~380 μm in diameter) isolated in the isotonic MIB solution had the wrinkled and rough NE (Figure S-1A). The swelling of the isolated nucleus in the hypotonic MIB solution of 5.5 g/L PVP expanded and smoothened the NE (~580 μm in diameter), which was detached from the white nucleoplasm (Figure S-1B). Noticeably, the self-standing NE of a swollen nucleus can selectively mediate the importin-facilitated transport of NLS-tagged BSA in the presence of 0.3 mM $FcTMA^+$ (Figure S-1C and D).

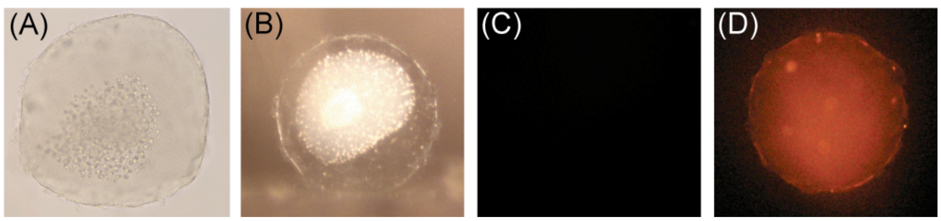


**Figure S-1.** Optical and video microscopic images of the nuclei isolated from *Xenopus laevis* oocytes in the (A) isotonic and (B) hypotonic MIB solutions, respectively. Fluorescence microscopic images of swollen nuclei in the hypotonic MIB solution of rhodamine-labeled and NLS-tagged BSA and 0.3 mM $FcTMA^+$ in the (C) absence and (D) presence of importins and energy mix.

**Fabrication of the SECM Cell.** The SECM cell (Figure 3A) was fabricated by sandwiching a 3 mm-diameter Si disk frame with a 0.5 mm × 0.5 mm aperture (frame thickness, 0.2 mm; Ted Pella, Redding, CA) between a pair of 5 mm × 5 mm Si frames with a 1.0 µm-thick $Si_3N_4$ membrane (frame thickness, 0.2 mm; membrane size, 0.5 mm × 0.5 mm; Norcada, Edmonton, Canada). The middle frame was glued to the bottom frame by applying M-Bond 610 adhesive (Ted Pella) and polished to reduce the thickness of the frame composite to 380 ± 5 µm as measured by a micrometer. A 10 µm × 10 µm opening was milled through the center of the $Si_3N_4$ membrane of the top Si frame by FIB and characterized by SEM (Figure S-2) using a dual-beam instrument (SMI3050SE FIB-SEM, Seiko Instruments, Chiba, Japan).

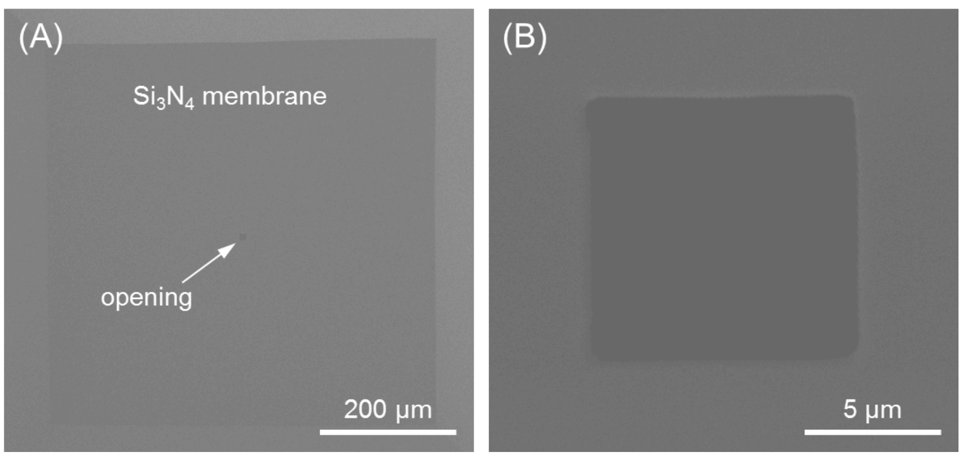


**Figure S-2.** SEM images of the 10 µm × 10 µm opening milled through the center of the $Si_3N_4$ membrane of the top Si frame by FIB.

**Preparation of the Nucleus Sample in the SECM Cell.** The isolated nucleus was transferred to the center of the cavity of the middle and bottom Si frames in the SECM cell (Figure 3A) filled with the isotonic MIB solution containing 15 g/L PVP and 0.3 mM $FcTMA^+$. The bottom frame was placed on the Plexiglass plate pretreated with 10 g/L of BSA (Sigma-Aldrich) at the 19 mm × 19 mm bottom part of a 12 mm-height Plexiglass cell. The two-thirds of the isotonic MIB solution was replaced with the MIB solution of 4.0 g/L PVP and 0.3 mM $FcTMA^+$ twice consecutively to dilute the PVP concentration to 5.5 g/L. The nucleus was swollen in the hypotonic MIB solution for 45 min. For SECM experiments with WGA, the swollen nucleus was incubated with the hypotonic MIB solution of 1.0 g/L WAG. Then, the top Si frame with a 10 μm × 10 μm opening was dropped on the top of the middle Si frame pretreated with 2 μL Cell-Tak (BD Biosciences, Bedford, MA) as a biological adhesive. The nucleus was swollen further for 15–20 min until the NE detached from the nucleoplasm and made contact with the $Si_3N_4$ membrane (Figure 3B).

**Fabrication and Characterization of the SECM Tip.** A ~0.5 µm-radius Pt tip surrounded by a ~0.5 µm-thick glass sheath was fabricated and characterized as reported elsewhere.[S-1] Briefly, a mechanically pulled Pt tip[S-2] was heat-annealed to thin the surrounding glass sheath and was milled by FIB to smoothen and flatten the tip end as confirmed by SEM and FIB imaging (Figure S-3A and 3B, respectively). In this work, a borosilicate glass capillary (1.0 mm outer diameter, 0.2 mm inner diameter, 200 mm length, Drummond Scientific Company, Broomall, PA) was used instead of a Pb-doped glass capillary to minimize the mechanical damage of the tip due to FIB milling. The FIB-milled tip gave a sigmoidal and nearly retraceable steady-state cyclic voltammogram of $FcTMA^+$ with a small capacitive current in the hypotonic MIB solution (Figure S-3C).

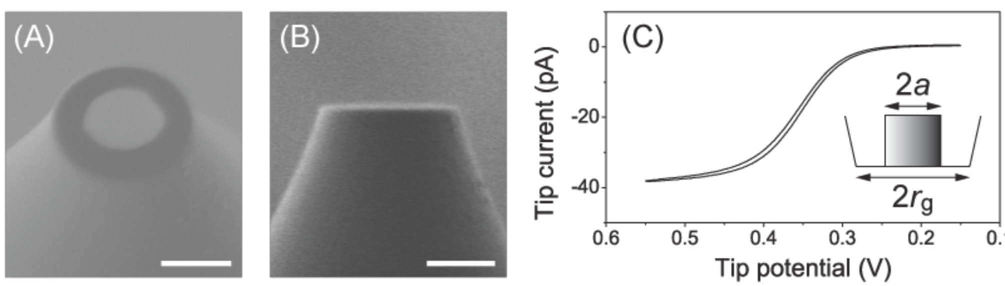


**Figure S-3.** (A) SEM and (B) FIB images of a FIB-milled Pt tip. Scale bars, 1 µm. (C) Cyclic voltammogram of 0.3 mM $FcTMA^+$ in the hypotonic MIB solution at a scan rate of 20 mV/s. The tip potential was defined against an Ag/AgCl reference electrode.

Remarkably, the small and sharp SECM tip was able to approach to a distance of ~25 nm from the flat $SiO_2$ substrate without the tip-substrate contact. This short distance was determined by fitting an experimental curve at the insulating substrate with the theoretical curve based on a negative feedback effect at an inlaid disk tip[S-3] (Figure S-4). The theoretical curve based on the hindered diffusion of $FcTMA^+$ to the tip is sensitive to *RG*.[S-4] A good fit of the experimental curve with the theoretical curve required $r_g$ = 0.92 μm (i.e., *RG* = 1.8) as determined by SEM in addition to $D_w = 5.4 \times 10^{-6}$ $cm^2$/s and *a* = 0.51 μm.

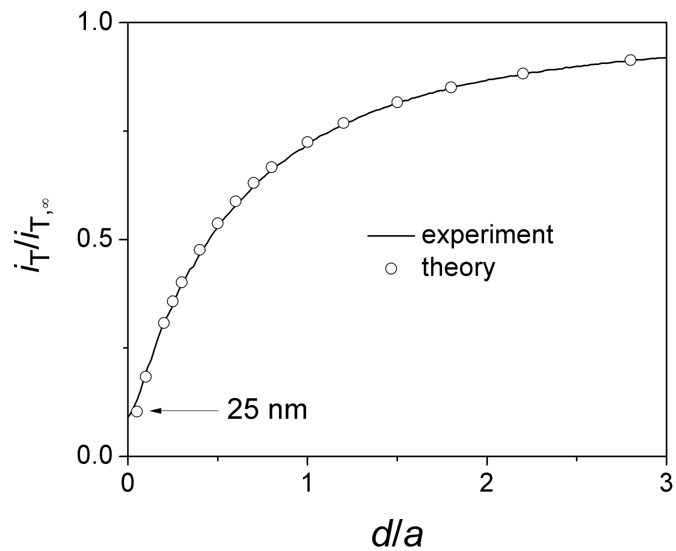


**Figure S-4.** Normalized SECM approach curve at the $SiO_2$-coated Si wafer in the hypotonic MIB solution of 0.3 mM $FcTMA^+$. Tip potential, 0.55 V against an Ag/AgCl reference electrode. Tip approach rate, 0.30 μm/s. The theoretical curve was calculated for *RG* = 1.8.[S-3]

**Finite Element Simulation.** In this work, the three-dimensional SECM diffusion problem was solved using COMSOL Multiphysics finite element package (version 3.5a, COMSOL, Burlington, MA). The finite element simulation employed normalized parameters as defined elsewhere[S-5] (see the attached exmple of the simulation). For instance, the normalized NE permeability was defined as

$$K = \frac{k_{\mathrm{NE}} a}{D_{\mathrm{w}}} \tag{S-1}$$

In Cartesian coordinates, the origin of the coordinate axes was set at the center of the NE exposed from the square opening. The $z$-axis was defined along the length of the tip (Figure S-5A). Actual simulations were carried out in a quarter of the entire domain because of symmetry planes at $x$ = 0 and $y$ = 0 (Figure S-5B). The diffusion of $\mathrm{FcTMA}^{+}$ in the outer solution and nucleus was defined by

$$\frac{\partial c_{\mathrm{w}}(x,y,z)}{\partial t} = D_{\mathrm{w}}\left[\frac{\partial^2 c_{\mathrm{w}}(x,y,z)}{\partial x^2} + \frac{\partial^2 c_{\mathrm{w}}(x,y,z)}{\partial y^2} + \frac{\partial^2 c_{\mathrm{w}}(x,y,z)}{\partial z^2}\right] \tag{S-2}$$

$$\frac{\partial c_{\mathrm{n}}(x,y,z)}{\partial t} = D_{\mathrm{w}}\left[\frac{\partial^2 c_{\mathrm{n}}(x,y,z)}{\partial x^2} + \frac{\partial^2 c_{\mathrm{n}}(x,y,z)}{\partial y^2} + \frac{\partial^2 c_{\mathrm{n}}(x,y,z)}{\partial z^2}\right] \tag{S-3}$$

where $c_{\mathrm{w}}(x, y, z)$ and $c_{\mathrm{n}}(x, y, z)$ are the concentrations of $\mathrm{FcTMA}^{+}$ in the respective sides of the NE. The diffusion coefficient, $D_{\mathrm{w}}$, and bulk concentraion, $c^{*}$, of $\mathrm{FcTMA}^{+}$ are identical at both sides of the NE. The tip reaction was limited by the diffusion of $\mathrm{FcTMA}^{+}$, which was depleted in the adjacent aqueous solution to induce its transport through the NPCs (Figure 2). The boundary condition at the NE was given by

$$D_w \left[ \frac{\partial c_w(x,y,z)}{\partial z} \right]_{z=0} = D_w \left[ \frac{\partial c_n(x,y,z)}{\partial z} \right]_{z=0} = k_{NE} \left[ c_w(x,y,0) - c_n(x,y,0) \right] \quad \text{(S-4)}$$

On the other hand, the $Si_3N_4$ membrane and the glass sheath of the tip were impermeable to $FcTMA^+$ to give zero flux across these boundaries. Boundary conditions at simulation space limits were given by the bulk concentration of $FcTMA^+$. The simulation space was large enough to give an error of less than 2% as estimated by comparing the simulated negative feedback current with the theoretical one in Figure 5B.

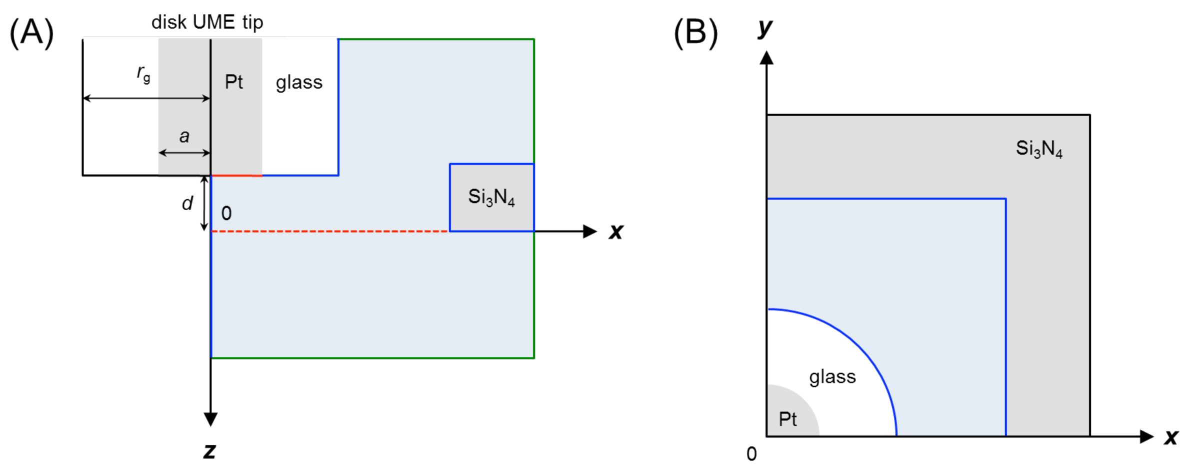


**Figure S-5.** Cross sections of the SECM geometry at (A) *xz* and (B) *xy* planes. In part (A), 4 types of boundary conditions are defined in the simulation space (light blue). The boundary condition at the NE (red dotted line) is given by eq S-4. The boundary condition at the tip (red solid line) is the diffusion-limited oxidation of $FcTMA^+$. There is no normal flux across the symmetry planes and impermeable surfaces (blue lines). Simulation space limits are shown by green lines.

**Derivation of Eq 3 for NE Permeability.** As reported elsewhere,[S-5] eq 3 was obtained from the following equation

$$k_{\mathrm{NE}} = \frac{k_1 k_2}{k_1 + 2k_2} \qquad \text{(S-5)}$$

where $k_1$ is based on the diffusion of $FcTMA^+$ between the orifice of the nanopore and the adjacent solution, i.e., steps (i) and (iii) in Figure 6A, and $k_2$ is based on the diffusion of $FcTMA^+$ through the nanopore, i.e., step (ii). When nanopores are randomly distributed, effective medium theories based on Brownian dynamics simulations give[S-6]

$$k_1 = 4D_{\mathrm{w}} Nrf(\sigma) \qquad \text{(S-6)}$$

Assuming the planar diffusion of $FcTMA^+$ through the NPCs, we defined $k_2$ as

$$k_2 = \frac{\pi r^2 N D_{\mathrm{NPC}}}{l} \qquad \text{(S-7)}$$

The combination of eq S-5 with eq S-6 and eq S-7 gives

$$k_{\mathrm{NE}} = \frac{2ND_{\mathrm{w}} r}{2lD_{\mathrm{w}} / \pi r D_{\mathrm{NPC}} + 1/f(\sigma)} \qquad \text{(S-8)}$$

This equation was used to evaluate $k_{\mathrm{NE}}$ values in the third and fourth rows of Table 1, where $D_{\mathrm{w}} = 3D_{\mathrm{NPC}}$. Eq S-8 with $D_{\mathrm{w}} = D_{\mathrm{NPC}}$ is equivalent to eq 3.

## REFERENCES

(S-1) Nioradze, N.; Kim, J.; Amemiya, S. *Anal. Chem.* **2011**, *83*, 828.

(S-2) Sun, P.; Mirkin, M. V. *Anal. Chem.* **2006**, *78*, 6526.

(S-3) Cornut, R.; Lefrou, C. *J. Electroanal. Chem.* **2007**, *604*, 91.

(S-4) Shao, Y.; Mirkin, M. V. *J. Phys. Chem. B* **1998**, *102*, 9915.

(S-5) Ishimatsu, R.; Kim, J.; Jing, P.; Striemer, C. C.; Fang, D. Z.; Fauchet, P. M.; McGrath, J. L.; Amemiya, S. *Anal. Chem.* **2010**, *82*, 7127.

(S-6) Makhnovskii, Y. A.; Berezhkovskii, A. M.; Zitserman, V. Y. *J. Chem. Phys.* **2005**, *122*, 236102.